Journal of Alloys and Compounds 509 (2011) 262–265

Contents lists available at ScienceDirect

Journal of Alloys and Compounds

journal homepage: www.elsevier.com/locate/jallcom

Optical and structural properties of nanostructured CeO_2:Tb^{3+} film

Anees A. Ansari*, S.P. Singh, B.D. Malhotra

National Physical Laboratory, Dr. KS Krishnan Marg, New Delhi 110012, India

ARTICLE INFO

Article history:
Received 8 January 2010
Received in revised form 30 June 2010
Accepted 6 July 2010
Available online 14 July 2010

Keywords:
Nanostructured CeO_2:Tb^{3+} film
Scanning electron microscopy
UV/Vis
Photoluminescence

ABSTRACT

Nanostructured CeO_2:Tb^{3+} film has been fabricated on glass substrate through sol–gel technique via dip-coating process. $(NH_4)_2Ce(NO_3)_6$, $Tb(NO_3)_3{\cdot}6H_2O$, ethylene glycol have been used as precursors for sol preparation. X-ray diffraction (XRD), scanning electron microscopy (SEM), UV/VIS and photoluminescence (PL) spectral studies have been employed to analyze the structural and optical properties of the film. XRD pattern has been used to analyze the crystallite nature and calculated particle size by Scherrer equation of nanostructured CeO_2:Tb^{3+} film, found in the range 3–4 nm. SEM image has been observed to analyze the surface topography of the film which is well porous, highly agglomerated and uniformly distributed nanoparticles on the film surface. Optical band gap of nanostructured CeO_2:Tb^{3+} film has been estimated as 3.57 eV. A significant enhancement in band shape of CeO_2:Tb^{3+} spectrum has been observed in PL spectra, showed their promising usages as optical materials in optoelectronic devices.

1. Introduction

Recently, luminescent metal ions doped cerium oxide nanophosphors with a narrow size distribution (<10 nm) and high luminescent efficiencies are of great importance because of their applications in high-performance luminescent devices, biological fluorescence labeling, luminescent paints and inks for security codes [1–4]. Because, these metal oxide nanophosphors possess higher chemical and thermal stability than commonly used mixed metal alloy phosphors such as ZnS:Cu, Al and Y_2O_2S:Eu^{3+} [5,6]. This advantage make them highly attractive for the application of laser materials due to these materials are chemically more stable in high vacuum and under electron excitation. Therefore, it is a continuous search to develop new oxide nanophosphor materials with high performance for phosphor applications.

Generally rare earth (RE) ions based on intra-configurational electronic transitions show sharp spectral transitions in visible region arising from their 4f electrons [1,7,8]. When combined with ultra-violate light emitting diode (UVLEDs), phosphors should be in a thin-film form and provide advantages such as high emission efficiencies, good compatibility with semiconductor devices and low fabrication cost. Furthermore, the excitation at near-ultraviolet wavelength is preferable to the use of LEDs as light sources. In contrast to rare earth doped nanophosphors such as $CePO_4$:RE, Y_2O_3:RE, CeF_3:RE or $NaYF_4$:RE, RE doped cerium oxide films in view of luminescence has been relatively less studied [9–13]. Tetravalent cerium ions (Ce^{4+}) have no 4f electron. This implies that CeO_2 can be a promising photoluminescence host material because of strong light absorption through the charge transfer (CT) from O^{2-} to Ce^{4+} [1–8].

In recent years some attempt have been performed for the preparation of RE ion doped cerium oxide by various techniques such as pyrolysis [4], solvothermal synthesis [2,14], sonochemical synthesis [15], the two-stage co-precipitation process [16,17], sol–gel process [1,8], solid-state ceramic reactions [18], microwave irradiation [19] and so on [14–22]. Relatively few reports are based on structural and optical properties of RE ions doped CeO_2 [1,15–19]. Fujihara et al., used spin-on/pyrolysis method for deposition of luminescent thin films of Eu^{3+} and Sm^{3+} doped CeO_2 on quartz glass substrate [4].

In the present article, we report sol–gel derived nanostructured Tb^{3+} doped CeO_2 film deposited on glass substrate and studies their optical characteristics at temperature.

2. Experimental

2.1. Chemicals and reagents

All chemicals used for the fabrication of CeO_2:Tb^{3+} film including ammonium cerium nitrate $(NH_4)_2Ce(NO_3)_6$, terbium nitrate $Tb(NO_3)_3{\cdot}6H_2O$ and ethylene glycol were analytical grade and procured from E-Merck India Ltd, Mumbai, India. Borosil glass plates were procured from Borosil Mumbai, India. The deionized water obtained from Millipore water purification system (Milli Q 10 TS) was used for the preparation of solution.

2.2. CeO_2:Tb^{3+} film preparation

CeO_2:Tb^{3+} film was fabricated on glass substrate by the literature method with little modification [23]. $Ce(NO_3)_3{\cdot}6H_2O$ and terbium nitrate $Tb(NO_3)_3{\cdot}6H_2O$ were used as precursor for film fabrication. 1:10 molar ratios of terbium and cerium nitrate precursor solutions were added into ethylene glycol at room temperature. A semi-

* Corresponding author. Tel.: +91 11 45609152; fax: +91 11 45609310.
E-mail address: aneesaansari@gmail.com (A.A. Ansari).

0925-8388/$ – see front matter © 2010 Elsevier B.V. All rights reserved.
doi:10.1016/j.jallcom.2010.07.009

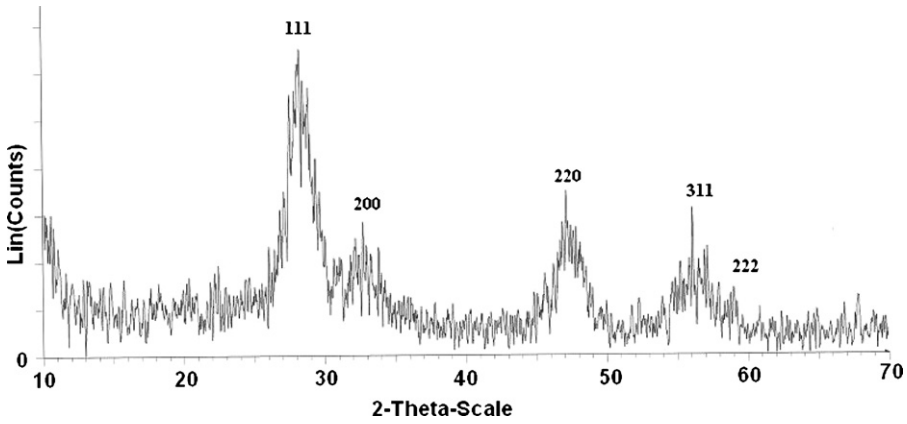

Fig. 1. X-ray diffraction pattern of nanostructured CeO_2:Tb^{3+} film.

transparent viscous gel was obtained for film fabrication on glass substrate. The film was deposited on glass substrate using dip-coating technique with a selected pulling speed of 10 cm/min. The prepared film was dried in air at room temperature and afterward annealed at 600 °C for 30 min.

2.3. Characterization

X-ray diffraction (XRD, Cu Ka radiation (Rigaku)) study was performed to identify the crystal structure of sol–gel derived CeO_2:Tb^{3+} film. Scanning electron micrograph (SEM), LEO-440 was used to examine the surface morphology of CeO_2:Tb^{3+} film. Optical absorption spectra of bulk CeO_2 and nanostructured CeO_2:Tb^{3+} film was recorded on Shimadzu UV-2100 spectrophotometer in the wavelength range 200–600 nm (Bulk CeO_2 powder was dispersed in ethanol for film fabrication on glass substrate via drop casting method). Photoluminescence (PL) spectra were measured at room temperature with a spectrophotometer (Perkin Elmer L-55).

3. Results and discussion

Fig. 1 shows results of X-ray diffraction studies carried out on nanostructured CeO_2:Tb^{3+} film deposited on glass substrate through sol–gel chemical process in 2θ range 20–70°. The results of XRD pattern indicate that terbium doped CeO_2 film is well crystalline and reveals five distinct diffraction peaks corresponding to (1 1 1), (2 0 0), (2 2 0) and (3 1 1) planes, which are perfectly similar to the JCPDS data (Card No. 34-0394) [2,4,24]. The broadening of diffraction peaks in the diffractogram confirms the nanocrystalline nature of the deposited CeO_2:Tb^{3+} film [2,24]. According to the Scherrer equation, the strongest peak (1 1 1) at $2\theta = 28.4°$ and (2 2 0) at $2\theta = 47.17°$ are used to calculate the average grain size of CeO_2:Tb^{3+} film to be 3–4 nm. The lattice constant (a) for the nanostructured CeO_2:Tb^{3+} film also calculated from peak position and its value found to be 0.544 nm, which is little high to the reported value for bulk CeO_2 (0.5411 nm). The calculated value of lattice constant is reasonably found high due to successful doping of Tb^{3+} ion into the CeO_2 crystal lattice [25–27]. In addition, the broadening in the XRD reflection planes owing to the increased lattice defect and disorder formation induced by doping [2,4]. Lin et al. reported increase lattice constant value due to the lattice expansion effect resulting from increase oxygen vacancies and Ce^{3+} ions with decreasing particle size [28].

Scanning electron micrograph was used to analyze the surface texture of deposited film of sol–gel derived nanostructured CeO_2:Tb^{3+} film assembled on glass substrate (Fig. 2). SEM image shows the film is well porous, homogenous, and spherical nanoparticles are uniformly distributed with well interconnected to each other.

Fig. 3 exhibits the UV/Vis spectra of nanostructured CeO_2:Tb^{3+} film with bulk CeO_2 film. The absorption spectrum of nanostructured CeO_2: Tb^{3+} film shows a broad band with maxima at 301 nm.

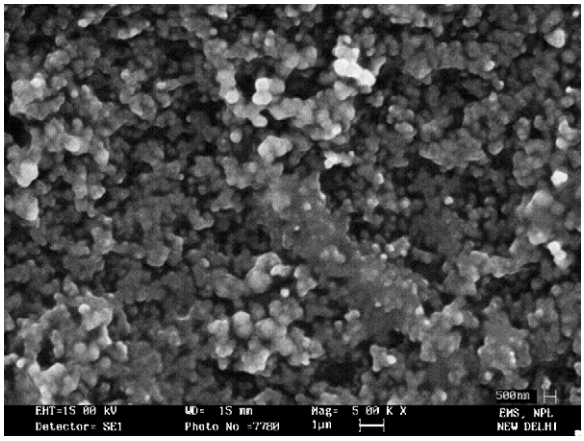

Fig. 2. SEM micrographs of nanostructured CeO_2:Tb^{3+} film.

The absorption edge of nanostructured CeO_2:Tb^{3+} spectrum shifts toward shorter wavelength in respect to bulk CeO_2 indicates that the grain size of nanostructured film is decreases. This kind of blue shifting phenomenon in absorption spectrum of nanocrystalline CeO_2 material has been discussed in literature by many investigators [2,13,29].

Optical band gap (E_g) of nanostructured CeO_2:Tb^{3+} film was estimated using the equation for semiconductor: $\alpha h\nu = C(h\nu - E_g)^n$

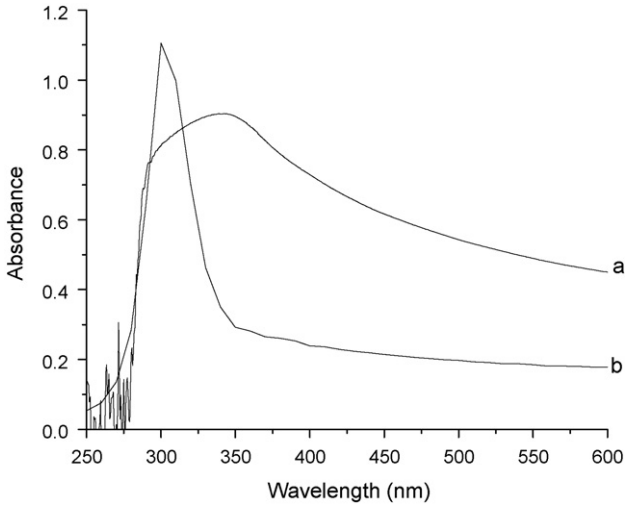

Fig. 3. Absorption spectra of (a) bulk CeO_2 film (b) nanostructured CeO_2:Tb^{3+} film.

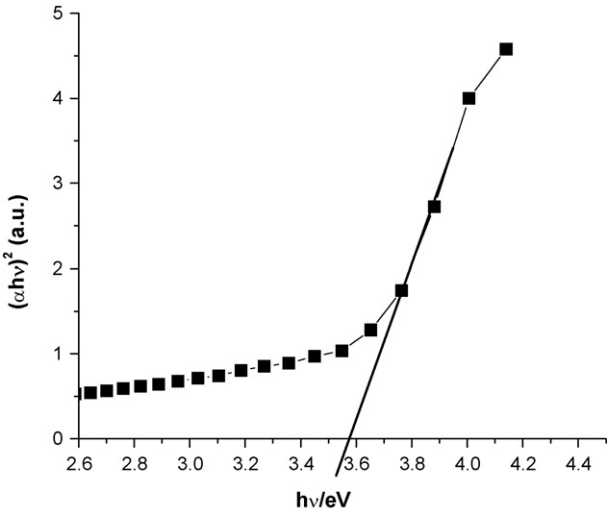

Fig. 4. Plot of $(\alpha h\nu)^2$ as a function of photon energy, E_d, for the nanostructured CeO_2:Tb^{3+} film.

where, α is the absorption coefficient, $h\nu$ is photon energy, C is the constant, $n = 1/2$ for a directly allowed transition, and $n = 2$ for an indirectly allowed transition. Optical absorption coefficient α is calculated according to the equation $\alpha = (2.303 \times 10^3 A\rho)/lc$, where A is the absorbance of a sample, ρ is the real density of CeO_2 (7.28 g cm^{-3}), l is the path length, and c is the concentration of the cerium oxide. Fig. 4 shows the plot of $(\alpha h\nu)^2$ versus photon energy for nanostructured CeO_2:Tb^{3+} film. The absorption edge of present nanocrystalline CeO_2:Tb^{3+} film (E_d) (3.57 eV) is blue-shifted evidently compared with that of the reported value (E_d) (3.15 eV), which is mainly resulted from quantum confinement effect [2,13]. Yin et al. concluded that the blue shift of absorption peak and absorption edges in the UV–vis absorption spectrum result from the quantum size effect [30].

Photoluminescence properties of nanostructured CeO_2:Tb^{3+} film along with bulk part CeO_2 film were investigated by measuring the emission (Excitation 220 nm) spectra (Fig. 5). The spectrum of nanostructured CeO_2:Tb^{3+} film exhibits a broad band in blue-green region (maxima at 390 nm), which is almost similar to the undoped CeO_2 spectrum. It is found that the emission band in doped film is dominant and gradually shifts toward longer wavelength. This significant enhancement in the emission band of doped film spectrum may be due to doping effect of Tb^{3+} ion in CeO_2 matrix. This characteristic emission band is already assigned as intra-configurational Ce^{4+}–O^{2-} charge transfer (CT) transition in undoped CeO_2 by Danielson et al. [31,32]. A comparison of these two spectrum strongly suggest that emission is achieved through charge transfer between the O_2 valence band and Ce^{4+} conduction band and subsequent energy transfer to Tb^{3+}. The molar absorption coefficient of Ce^{4+} is very high when compared with that of Tb^{3+} and Tb^{3+} is substituted at the Ce^{4+} site, it is possible that the CT band of Ce^{4+} inhibit the CT band of Tb^{3+} in this lattice. In luminescent materials, energy transfer mechanism between ions of the same or different types and between the host and the activator are well known. They are either due to resonance or exchange interaction or multipolar interaction between the ions of the same or different type, which deepens on the critical energy transfer distance (Rc) between the absorbing group in the crystal lattice. The energy absorbed by the CT from O^{2-} valence band to Ce^{4+} conduction band is transferred to the Tb^{3+} and produces the blue-green emission. The energy level of Tb^{3+} (^4f_n) in CeO_2:Tb^{3+} nanocrystalline film is suitable to accept energy from the excited state of Ce^{4+} following the allowed f–d transition upon its excitation with UV light [2,4,24]. This might result from the large quantity of CeO_2 existing on the film surface, which quenched the fluorescence emission of Tb^{3+} to a large extent. Therefore, characteristic 4f–4f emission transitions of Tb^{3+} detected in nanostructured CeO_2:Tb^{3+} film spectrum might be due to small concentration of terbium ion in the film (Fig. 5). So far, few studies on PL of CeO_2 have been reported.

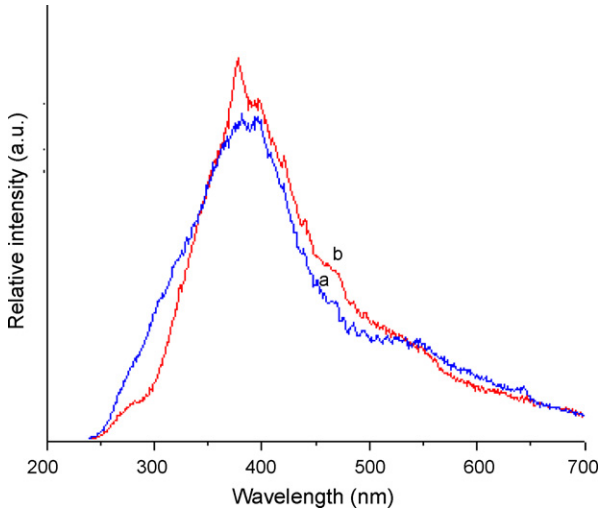

Fig. 5. Photoluminescence spectra (a) bulk CeO_2 film (b) nanostructured CeO_2:Tb^{3+} film.

4. Conclusions

Sol–gel derived nanostructured CeO_2:Tb^{3+} film was fabricated on glass substrate through dip-coating process using cerium ammonium nitrate, terbium nitrate and ethylene glycol as precursors. The average grain size of nanostructured film was estimated by Scherrer equation as 3–4 nm. Optical absorption band of CeO_2:Tb^{3+} film exhibit blue shift in respect to their bulk counterpart (CeO_2 film). Absorption spectral results indicated that the direct band gap of CeO_2:Tb^{3+} (3.57 eV) decreases as the particle size decrease. A significant enhancement in PL intensity suggests the successful doping of Tb^{3+} ion in nanostructured CeO_2:Tb^{3+} film. Efforts should be made to improve the quality of the film for application to luminescent device fabrication and solar cell materials.

Acknowledgements

Author (AAA) thanks CSIR for financial support and Director of NPL, New Delhi, India for providing experimental facilities, which is gratefully acknowledge.

References

[1] L. Li, H.K. Yang, B.K. Moon, Z. Fu, C. Guo, J.H. Jeong, S.S. Yi, K. Jang, H.S. Lee, J. Phys. Chem. C 113 (2009) 610.
[2] Z. Wang, Z. Quan, J. Lin, Inorg. Chem. 46 (2007) 5237.
[3] X.H. Liu, S. Chen, X. Wang, J. Lumin. 127 (2007) 650.
[4] S. Fujihara, F M., J. Appl. Phys. 95 (2004) 8002.
[5] R. Raue, M. Shiiki, H. Matsukiyo, H. Toyama, H.Y. Yamamoto, J. Appl. Phys. 75 (1994) 481.
[6] S. Itoh, M. Yokoyama, K.J. Morimoto, J. Vac. Sci. Technol. A 5 (1987) 3430.
[7] A.A. Ansari, N. Singh, A.F. Khan, S.P. Singh, Lumin J. 127 (2007) 446.
[8] A.A. Ansari, J. Semiconduct. 31 (2010).
[9] B.K. Gupta, D. Haranath, S. Saini, V.N. Singh, V. Shanker, Nanotechnology 21 (2010) 055607.
[10] L. Li, M. Zhao, W. Tong, X. Guan, G. Li, L. Yang, Nanotechnology 21 (2010) 195601.
[11] F. Zhang, J. Li, J. Shan, L. Xu, D. Zhao, Chem. Eur. J. 15 (2009) 1010.
[12] H. Schafer, P. Ptacek, H. Eickmeier, M. Haase, Adv. Funct. Mater. 19 (2009) 3091.
[13] A.A. Ansari, N. Singh, S.P. Singh, J. Nanopart. Res. 10 (2008) 703.
[14] T. Karaca, T.G. Altıncekic, M.F. Oksuzomer, Ceram. Int. 36 (2010) 1101.
[15] E.C.C. Souza, H.F. Brito, E.N.S. Muccillo, J. Alloys Compd. 491 (2010) 460.

[16] E.C.C. Souza, E.N.S. Muccillo, J. Alloys Compd. 473 (2009) 560.
[17] M. Llusar, L. Vitaskova, P. Sulcova, M.A. Tena, J.A. Badenes, G. Monros, J. Eur. Ceram. Soc. 30 (2010) 37.
[18] P.S. Anjana, T. Joseph, M.T. Sebastian, J. Alloys Compd. 490 (2010) 208.
[19] Y.P. Fu, Ceram. Int. 35 (2009) 653.
[20] S. Xinyuan, G. Mu, Z. Min, H. Shiming, J. Rare Earths 28 (2010) 340.
[21] L. Zeng, D. Chen, L. Cui, F. Huang, Y. Wang, Scripta Mater., doi:10.1016/j.scriptamat.2010.05.033.
[22] S. Babu, A. Schulte, S. Seal, Appl. Phys. Lett. 92 (2008) 123112.
[23] T. Suzuki, I. Kosacki, H.U. Anderson, J. Am. Ceram. Soc. 85 (2002) 1492; T. Suzuki, I. Kosacki, H.U. Anderson, Solid State Ionics 151 (2002) 111.
[24] S. Patil, S. Seal, Y. Guo, A. Schulte, J. Norwood, Appl. Phys. Lett. 88 (2006) 243110.
[25] D. Vander Voort, J.M.E. Rijk, R.V. Doorn, G. Blasse, Mater. Chem. Phys. 31 (1992) 333.
[26] J. Alarcon, D.V. Voort, G. Blasse, Mater. Res. Bull. 27 (1992) 467.
[27] A.H. Morhed, M.E. Moussa, S.M. Bedair, R. Leonard, S.X. Liu, N.A. El-Masry, Appl. Plys. Lett. 75 (1997) 2389.
[28] Y.S. Lin, Y. Hung, H.Y. Lin, Y.H. Tseng, Y.F. Chen, C.Y. Mou, Adv. Mater. 19 (2007) 577.
[29] T. Masui, K. Fujiwara, K. Machida, G. Adachi, Chem. Mater. 9 (1997) 2197.
[30] L.X. Yin, Y. Wang, G. Pang, Y. Koltypin, A. Gedanken, J. Coll. Inter. Sci. 246 (2002) 78.
[31] E. Danielson, M. Devenney, D.M. Giaquinta, J.H. Golden, R.C. Haushalter, E.W. McFarland, D.M. Poojary, C.M. Reaves, W.H. Weinberg, X.D. Wu, Science 279 (1998) 837.
[32] E. Danielson, J.H. Golden, E.W. McFarland, C.M. Reaves, W.H. Weinberg, X.D. Wu, Nature 389 (1997) 944.